

# Simulation of dendritic growth of magnesium alloys with fluid flow

\*Meng-wu Wu<sup>1,2</sup>, Zhi-peng Guo<sup>3</sup> and Shou-mei Xiong<sup>3</sup>

1. Hubei Key Laboratory of Advanced Technology for Automotive Components, Wuhan University of Technology, Wuhan 430070, China;

2. Hubei Collaborative Innovation Center for Automotive Components Technology, Wuhan 430070, China;

3. School of Materials Science and Engineering, Tsinghua University, Beijing 100084, China

**Abstract:** Fluid flow has a significant impact on the microstructure evolution of alloys during solidification. Based on the previous work relating simulation of the dendritic growth of magnesium alloys with hcp (hexagonal close-packed) structure, an extension was made to the formerly established CA (cellular automaton) model with the purpose of studying the effect of fluid flow on the dendritic growth of magnesium alloys. The modified projection method was used to solve the transport equations of flow field. By coupling the flow field with the solute field, simulation results of equiaxed and columnar dendritic growth of magnesium alloys with fluid flow were achieved. The simulated results were quantitatively compared with those without fluid flow. Moreover, a comparison was also made between the present work and previous works conducted by others. It can be concluded that a deep understanding of the dendritic growth of magnesium alloys with fluid flow can be obtained by applying the present numerical model.

**Key words:** magnesium alloy; dendritic growth; cellular automaton method; fluid flow

CLC numbers: TP391.99

Document code: A

Article ID: 1672-6421(2017)05-359-06

As the lightest known structural metals, magnesium alloys are treated as the green engineering materials of the 21st century due to their superior properties such as low density, high specific strength, excellent castability, good machinability and recyclability<sup>[1]</sup>. Magnesium alloys have been widely used in automotive, aerospace and 3C (computer, communication and consumer electronics) industries to replace steel, cast iron and even aluminum alloy. Such components and parts include steering wheels, gear boxes, notebook shells and mobile phone frames, etc.<sup>[2]</sup>. The performance of magnesium alloy parts is strongly influenced by the microstructure formed during solidification. Since the fluid flow has a significant impact on the structure formation of alloys during solidification<sup>[3]</sup>, and dendritic structure is probably the most commonly observed structure of magnesium alloys<sup>[4]</sup>, studying the effect of

fluid flow on the morphology and distribution of the dendritic structure of magnesium alloys is therefore very meaningful to control the microstructure formation, and consequently improve the properties of magnesium alloy parts.

In recent years, numerical modeling and simulation have been rapidly developed as a powerful tool for predicting the time-dependent microstructure evolution during various solidification processes<sup>[5,6]</sup>. Among those numerical modeling techniques, the CA method and PF (phase field) method have been extensively used as they both have the capability of predicting and depicting the evolution of complex solidification structures. For the dendritic growth of cubic metals, numerous simulation works have been reported<sup>[7-11]</sup>, whereas few have been done for the dendritic growth of magnesium alloys with hcp crystal structure. Using the PF method, Böttger et al.<sup>[12,13]</sup> and Wang et al.<sup>[14]</sup> successfully simulated the dendritic growth of magnesium alloys, reproducing most of the dendritic features observed experimentally. Yuan et al.<sup>[15]</sup> simulated the dendritic growth of magnesium alloy AZ91D with forced fluid flow, but the simulated dendrite morphology only revealed the growth of primary trunks, and the evolution of secondary dendrite

## \*Meng-wu Wu

Male, born in 1984, Ph.D. Research interests: simulation of casting and solidification processes of aluminum and magnesium alloys, including defect formation and microstructure evolution.

E-mail: wumw@whut.edu.cn

Received: 2017-08-15; Accepted: 2017-09-04

arms was not observed. Guo et al.<sup>[16]</sup> and Yao et al.<sup>[17]</sup> accurately depicted the dendrite morphology of magnesium alloys with primary trunks and secondary dendrite arms, while all of them revealed a six-fold symmetry morphology. Meanwhile, in their simulation works considering the effect of fluid flow on dendritic growth, conclusions were made that the growth velocity of dendrite tips at the upstream side was much faster than that at the downstream side. Due to the requirement of a small cell size with respect to the thickness of the solid/liquid interface and the consequent massive computational power, the PF method is limited to a small calculation domain. Another drawback of the PF method is that some of the parameters do not have direct correlation with physical data, such as diffusion coefficients and mobility parameter. Compared to the PF method, the CA method has attractive advantages such as simplicity of formulation and computational convenience when implemented to solve phase transition problems with an acceptable computational efficiency. However, modeling of dendritic growth of magnesium alloys with fluid flow based on the CA method is still rarely reported at present.

In this paper, a numerical model was established coupling the CA model with the continuity and Navier-Stokes equations to simulate the equiaxed and columnar dendritic growth of magnesium alloys with fluid flow. The effect of fluid flow on the dendritic growth of magnesium alloys with different growth orientations was investigated qualitatively and quantitatively in case studies. Moreover, a comparison was also made between the present work and previous works conducted by others.

## 1 Numerical model and algorithms

### 1.1 Momentum and mass transport

Fluid flow during solidification is treated as incompressible fluid flow. Here, the momentum and mass transport of fluid flow is controlled by the continuity and Navier-Stokes equations written as follows.

Equation of continuity is

$$\nabla \cdot \mathbf{u} = 0 \quad (1)$$

Navier-Stokes equation is

$$\rho \left( \frac{\partial \mathbf{u}}{\partial t} \right) + \rho (\mathbf{u} \cdot \nabla) \mathbf{u} + \nabla P = \mu \nabla^2 \mathbf{u} + S \quad (2)$$

where  $\mathbf{u}$  is the velocity of the fluid flow,  $t$  is the time,  $\rho$  is the density which is considered to be constant in liquid and solid phases,  $P$  is the hydrostatic pressure,  $\mu$  denotes the viscosity, and  $S$  is a source term via which the buoyancy force is taken into account. Compared to the forced fluid flow, the effect of buoyancy force on fluid flow is negligible, so the source term  $S$  is not considered during the calculation with forced fluid flow in this paper.

### 1.2 Solute transport

During the solidification of magnesium alloys, the solute redistribution plays an important role in determining the grain growth morphology and the corresponding microstructure characteristics. In the present work, the magnesium alloys were treated as binary alloys for simplification. As the solidification proceeds, the solute accumulates at the solidification front due to the solute rejection associated with the solidification of  $\alpha$ -Mg. And then, the solute redistribution is governed by both diffusion and convection in the whole domain. Therefore, the governing equations for solute redistribution in the solid and liquid are given by:

$$\frac{\partial c_s}{\partial t} = \nabla \cdot (D_s \nabla c_s) \quad (3)$$

$$\frac{\partial c_l}{\partial t} + \mathbf{u} \cdot \nabla c_l = \nabla \cdot (D_l \nabla c_l) + c_l (1 - k_0) \frac{\partial f_s}{\partial t} \quad (4)$$

where  $c_l$  and  $c_s$  are the solute concentrations of the liquid and solid, respectively.  $D_l$  and  $D_s$  are the liquid and solid solute diffusion coefficients.  $k_0$  is the solute partition coefficient, while  $f_s$  denotes the solid fraction. The last term on the right hand side of Eq. (4) represents the solute rejection at the solid/liquid interface due to the increment of the solid fraction of  $\alpha$ -Mg.

### 1.3 Growth kinetics and capturing rules

Based on the fact that Mg has a hcp crystal structure, the dendrites of commercially available magnesium alloys grow with six-fold symmetry in the basal plane  $\{0001\}$ . In the present paper, based on the CA method, a growth model was established in which the growth kinetics were calculated from the complete solution of the transport equations. By defining a special neighbourhood configuration with the square CA cell, and using a set of capturing rules which was proposed by Beltrán-Sánchez and Stefanescu for the dendritic growth of cubic crystal metals during solidification<sup>[10]</sup>, modeling of dendritic growth of magnesium alloy with six-fold symmetry and different growth orientations was achieved. More details relating calculation of the growth kinetics (including the growth velocity, solid fraction increment and mean curvature of the interface cells, etc.) and the capturing rules can be found in references [18,19].

## 2 Solution scheme of numerical model

In order to predict the dendritic growth of magnesium alloys with fluid flow, the CA model was coupled with a transport model for calculating solute transfer by both convection and diffusion during solidification. The continuity and momentum equations, Eqs. (1) and (2), were solved by the modified projection method based on the staggered grids<sup>[20]</sup>. An explicit finite difference scheme was employed for solving the time-dependent terms of Navier-Stokes equation, Eq. (2), and the species conservation equations, Eqs. (3) and (4). Both convection and diffusion terms were evaluated by the hybrid scheme.

Since the solutal diffusivity is usually several orders of magnitude smaller than the thermal diffusivity, a zero-flux boundary condition was imposed for solute transfer at four surfaces of the calculation domain. To simulate the dendritic growth of magnesium alloys with fluid flow, a forced incompressible Newtonian fluid flow was constructed that it entered the calculation domain through the left boundary with a uniform inlet velocity, and then exited the calculation domain from the right boundary. While the fluid flows past the solidified cells in the center, the solidified cells were assumed to be rigid and stationary. No slip boundary condition was applied at the solid-liquid interface. Moreover, the top and bottom surfaces

of the calculation domain were treated as the symmetrical boundaries for fluid flow.

### 3 Simulation results and discussion

Commercially available magnesium alloys AZ91 and AM60 were used in the case studies. The two alloys were treated as binary alloys for simplification, since the content of the remaining elements is extremely low except for the elements Mg and Al. The parameters and physical properties of the two alloys used in the present simulations are shown in Table 1<sup>[18,21]</sup>.

**Table 1: Physical property parameters of AZ91 and AM60 magnesium alloys<sup>[18,21]</sup>**

Parameter	AZ91	AM60
Initial mass fraction of Al, $C_0$ (%)	9.21	6.0
Liquidus temperature, $T_{l,eq}$ (K)	868	888
Solute partition coefficient, $k_0$	0.4	0.4
Liquidus slope, $k_l$ (K·% <sup>-1</sup> )	-6.59	-5.5
Solute diffusion coefficient in liquid, $D_l$ (m <sup>2</sup> ·s <sup>-1</sup> )	$1.8 \times 10^{-9}$	$1.8 \times 10^{-9}$
Solute diffusion coefficient in solid, $D_s$ (m <sup>2</sup> ·s <sup>-1</sup> )	$1.8 \times 10^{-12}$	$1.8 \times 10^{-12}$
Gibbs-Thomson's coefficient, $\Gamma$ (K·m)	$6.2 \times 10^{-7}$	$6.2 \times 10^{-7}$
Density, $\rho$ (kg·m <sup>-3</sup> )	$1.74 \times 10^3$	$1.74 \times 10^3$
Viscosity, $\mu$ (N·s·m <sup>-2</sup> )	$3.08 \times 10^{-3}$	$3.08 \times 10^{-3}$

#### 3.1 Equiaxed dendritic growth with fluid flow

In order to verify the present CA model, a simulation was conducted to simulate the dendritic growth of AZ91 magnesium alloy with forced fluid flow. A single nucleus was set at the center of the calculation domain which was divided into 400×400 square cells with a cell size of 2 μm. No further nucleation was considered then. A uniform temperature field with a cooling rate of 80 K·s<sup>-1</sup> was set at the calculation domain. Figure 1 shows the simulated equiaxed dendritic morphology of AZ91 magnesium alloy without fluid flow and with forced convection under a uniform inlet velocity of 0.1 mm·s<sup>-1</sup> from the left boundary of the calculation domain. According to Fig. 1(a), the dendrite is well-developed with six-fold symmetry under no fluid flow. Primary trunks and secondary dendrite arms grow along the direction  $\langle 11\bar{2}0 \rangle$  and form an angle of 60° with respect to each other. Moreover, the lengths of the primary trunks are almost identical. With forced convection as shown in Fig. 1(b), the dendrite reveals an asymmetrical morphology that the primary trunks and secondary dendrite arms at the upstream side grow faster and coarser than those at the downstream side. In other words, the growth of the dendrite trunks and side branching are all promoted at the upstream side and inhibited at the downstream side. It can be concluded that the simulated results are consistent with the experimental ones<sup>[22]</sup> and those simulated by the PF method<sup>[16,17]</sup>.

The effect of fluid flow on the growth velocity of the dendrite could be explained as follows: as the solidification proceeds, the solute atoms are rejected in the liquid ahead of the solid/liquid interface, and then washed away by the fluid flow from the upstream side to the downstream side, resulting in a lower solute concentration in the left region than that in the right region. According to the dendritic growth kinetics, the lower the solute concentration, the larger the local undercooling, and consequently the faster the growth velocity of the dendrite. An obvious evidence also can be found in Fig. 1(b) that the solute diffusion layer is much thinner at the upstream side than that at the downstream side, while the fluid flow is much weakened at the downstream side. A quantitative investigation was carried out to study the effect of the inlet velocity of fluid flow on the solute distribution at the dendrite tips as illustrated in Fig. 2. It can be noted that the quantitative results agree well with the qualitative analysis. A larger inlet velocity of the forced fluid flow leads to a steeper solute concentration gradient at the upstream dendrite tips, which consequently accelerates the dendritic growth of the magnesium alloy. At the downstream dendrite tips, when the inlet velocity increases, the solute concentration gradient decreases owing to a faster migration of the solute atoms from the upstream side to the downstream side. In this case, the dendritic growth will be much slower.

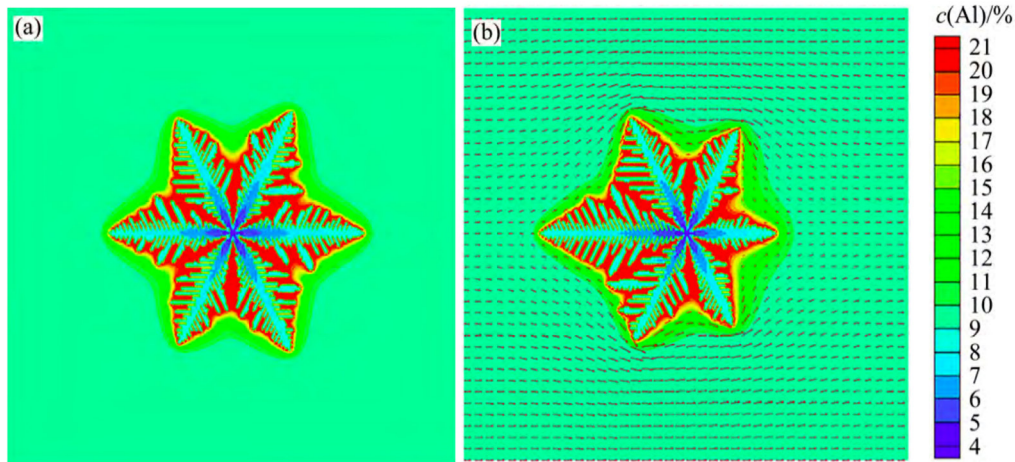


Fig. 1: Simulated equiaxed dendritic morphology of AZ91 magnesium alloy: (a) without fluid flow, (b) with forced convection under a uniform inlet velocity of  $0.1 \text{ mm}\cdot\text{s}^{-1}$

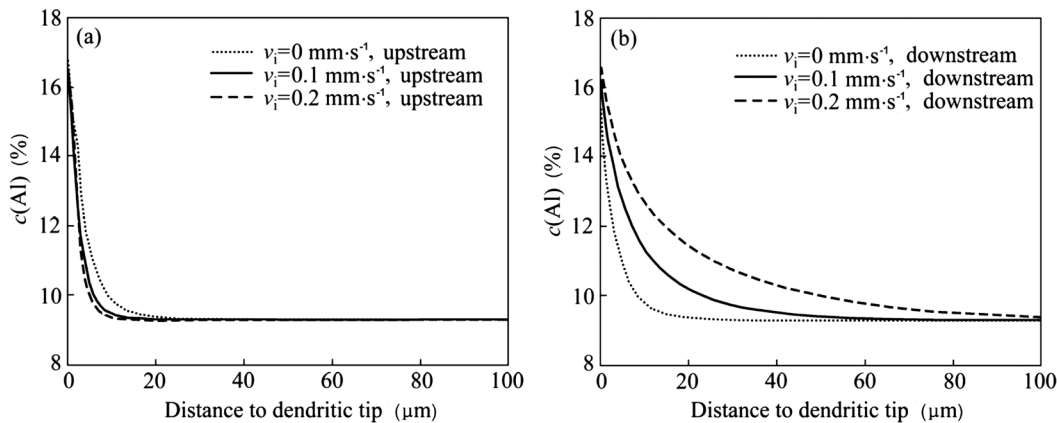


Fig. 2: Al concentration profiles of AZ91 magnesium alloy along horizontal direction with different inlet velocities of forced fluid flow: (a) at upstream dendrite tip, (b) at downstream dendrite tip

Simulations were further conducted to investigate the effect of fluid flow on the dendritic growth of multi-grain of AZ91 magnesium alloy with different growth orientations. Four nuclei with initial crystal orientations of  $0^\circ$  (left-bottom),  $15^\circ$  (left-top),  $30^\circ$  (right-bottom) and  $45^\circ$  (right-top) with respect to the direction of fluid flow were set at the calculation domain consisting of  $500 \times 500$  cells with a cell size of  $2 \mu\text{m}$ . Similarly, no further nucleation was taken into account. Assume that the temperature of the calculation domain was uniform and decreased at a cooling rate of  $80 \text{ K}\cdot\text{s}^{-1}$ . Figure 3 shows the simulated multi-dendrite growth of AZ91 magnesium alloy without fluid flow and with forced convection under a uniform inlet velocity of  $0.2 \text{ mm}\cdot\text{s}^{-1}$ . A remarkable difference relating the dendritic morphology can be seen compared Fig. 3(a) with 3(b).

According to Fig. 3(a), four dendrites with different growth orientations are all well-developed with coarse primary trunks and clearly visible secondary dendrite arms. Particularly, the lengths of the primary trunks are almost identical, not only in one certain dendrite but also among all the dendrites. As the solidification proceeds, the dendrites impinge on each other, which results in coarsening of the dendrites. However, the dendritic growth is quite different with forced convection as shown in Fig. 3(b). First, a similar conclusion can be made just

like before that the primary trunks and secondary dendrite arms at the upstream side grow faster and coarser than those at the downstream side in one dendrite. Meanwhile, the solute diffusion layer is much thinner at the upstream side than that at the downstream side. Second, comparing the growth morphology of the four dendrites, it can be noted that the "sweep" effect of fluid flow varies with different growth orientations of the dendrites. Take the left two dendrites for instance, the growth orientations are  $0^\circ$  (left-bottom) and  $15^\circ$  (left-top), respectively. The primary trunks at the most-upstream side are marked as " $g_0$ " and " $g_{15}$ ", while " $t_0$ ", " $b_0$ " and " $t_{15}$ ", " $b_{15}$ " are secondary dendrite arms branching on " $g_0$ " and " $g_{15}$ ", respectively. It can be seen that " $g_0$ " grows symmetrically, whereas " $g_{15}$ " reveals an asymmetrical morphology that " $t_{15}$ " grows stronger than " $b_{15}$ ". Meanwhile, " $t_{15}$ " is also more well-developed than " $t_0$ ". The cause of this phenomena can be described as follows: the "sweep" effect of fluid flow is the most intense when the dendrite trunks and arms grow along the direction parallel to the fluid flow. While there is an angle between the directions of the fluid flow and the dendrite trunks and arms, the "sweep" effect of fluid flow is weakened. Therefore, " $t_0$ " grows poorer than " $t_{15}$ " since a relative larger angle forms between " $t_0$ " and the direction of fluid flow than that of " $t_{15}$ ".

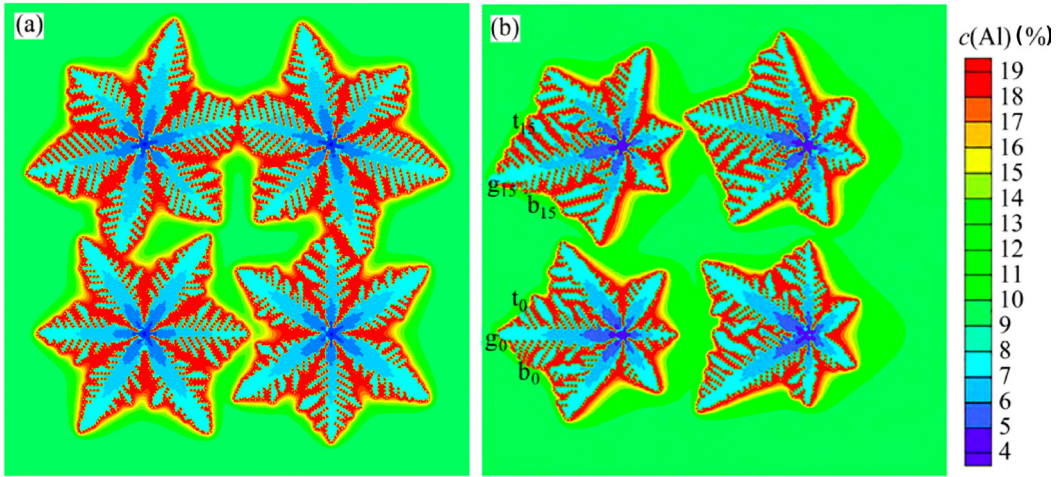


Fig. 3: Simulated multi-dendrite growth of AZ91 magnesium alloy: (a) without fluid flow, (b) with forced convection under a uniform inlet velocity of  $0.2 \text{ mm}\cdot\text{s}^{-1}$

### 3.2 Columnar dendritic growth with fluid flow

The present model was applied to simulate the columnar dendritic growth of AM60 magnesium alloy with fluid flow. Four nuclei with two different initial growth orientations were set at the bottom of the calculation domain consisting of  $300 \times 500$  cells with a cell size of  $2 \mu\text{m}$ . With a cooling rate of  $2.5 \text{ K}\cdot\text{s}^{-1}$  and a temperature gradient of  $10 \text{ K}\cdot\text{mm}^{-1}$  along the vertical direction of the calculation domain, Fig. 4 indicates the columnar dendritic growth of AM60 magnesium alloy without fluid flow and with forced convection under a uniform inlet velocity of  $0.05 \text{ mm}\cdot\text{s}^{-1}$ . It can be seen firstly both in Figs. 4(a) and (b) that among the four dendrites, the dendrite trunks and arms with their growth orientations aligned with the direction of the temperature gradient grew faster than the other dendrite trunks and arms under directional solidification. However, a relatively small difference relating the dendritic morphology could be observed by a careful comparison between Figs.

4(a) and (b). For the convenience of description, the four dendrites are marked as No. 1, 2, 3 and 4 from the left to the right as illustrated. Due to the effect of fluid flow, the growth of the primary trunk "l<sub>3</sub>" of dendrite No. 3 at the upstream side is promoted, while the growth of the primary trunk "r<sub>3</sub>" at the downstream side is inhibited. A similar situation occurs during the growth of the dendrite No. 1. Meanwhile, secondary dendrite arms branching on the left primary trunks of dendrites Nos. 2 and 4 are more well-developed, since a poorer growth of the right primary trunks of dendrites Nos. 1 and 3 offers a more sufficient space for solute diffusion. Generally speaking, the effect of fluid flow on the columnar dendritic growth is much weaker compared to that of the equiaxed dendritic growth, for the fluid flow is usually blocked and hindered by the nearby columnar dendrite. In such case, the "sweep" effect of fluid flow is weakened on the other columnar dendrites. It can be seen that the simulated results are in accordance with those simulated by Yuan et al. for the dendritic growth of Ni-Nb alloy<sup>[8]</sup>.

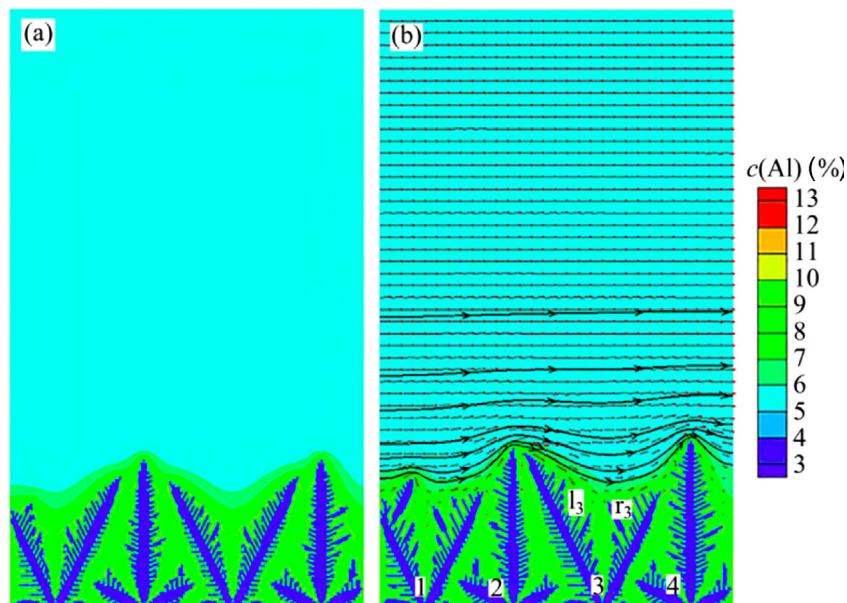


Fig. 4: Simulated columnar dendritic growth of AM60 magnesium alloy: (a) without fluid flow, (b) with forced convection under a uniform inlet velocity of  $0.05 \text{ mm}\cdot\text{s}^{-1}$

## 4 Conclusions

(1) A numerical model was established coupling the CA model with the continuity and Navier-Stokes equations to simulate the equiaxed and columnar dendritic growth of magnesium alloys with fluid flow. The capability of the present CA model was successfully verified by comparing the simulated results with the experimental ones and those simulated by the PF method. The simulated results indicate that the fluid flow has a profound impact on the dendritic growth of magnesium alloys.

(2) During the equiaxed dendritic growth of magnesium alloys with fluid flow, the dendrite reveals an asymmetrical morphology that the primary trunks and secondary dendrite arms at the upstream side grow faster and coarser than those at the downstream side. Meanwhile, a larger inlet velocity of the fluid flow leads to a steeper solute concentration gradient at the upstream dendrite tips, while the larger the inlet velocity, the smaller the solute concentration gradient at the downstream dendrite tips. Moreover, the "sweep" effect of fluid flow is the most intense when the dendrite trunks and arms grow along the direction parallel to the fluid flow. While there is an angle between the directions of the fluid flow and the dendrite trunks and arms, the "sweep" effect of fluid flow is weakened.

(3) The effect of fluid flow on the columnar dendritic growth is much weaker compared to that on the equiaxed dendritic growth, for the fluid flow is usually blocked and hindered by the nearby columnar dendrite.

## References

- [1] Kulekci M K. Magnesium and its alloys applications in automotive industry. *The International Journal of Advanced Manufacturing Technology*, 2008, 39(9): 851–865.
- [2] Joost W J, Krajewski P E. Towards magnesium alloys for high-volume automotive applications. *Scripta Materialia*, 2017, 128: 107–112.
- [3] Sun D, Zhu M, Pan S, et al. Lattice Boltzmann modeling of dendritic growth in a forced melt convection. *Acta Materialia*, 2009, 57(6): 1755–1767.
- [4] Yang M, Xiong S M, Guo Z. Effect of different solute additions on dendrite morphology and orientation selection in cast binary magnesium alloys. *Acta Materialia*, 2016, 112: 261–272.
- [5] Asta M, Beckermann C, Karma A, et al. Solidification microstructures and solid-state parallels: recent developments, future directions. *Acta Materialia*, 2009, 57(4): 941–971.
- [6] Allison J. Integrated computational materials engineering: a perspective on progress and future steps. *The Journal of The Minerals, Metals & Materials Society (JOM)*, 2011, 63(4):15–18.
- [7] Zhu M, Pan S, Sun D, et al. Numerical simulation of microstructure evolution during alloy solidification by using cellular automaton method. *ISIJ International*, 2010, 50(12): 1851–1858.
- [8] Yuan L, Lee P D, Djambazov G, et al. Numerical simulation of the effect of fluid flow on solute distribution and dendritic morphology. *International Journal of Cast Metals Research*, 2009, 22(1–4): 204–207.
- [9] Dong H B, Lee P D. Simulation of the columnar-to-equiaxed transition in directionally solidified Al-Cu alloys. *Acta Materialia*, 2005, 53(3): 659–668.
- [10] Beltran-Sanchez L, Stefanescu D M. A quantitative dendrite growth model and analysis of stability concepts. *Metallurgical and Materials Transactions A*, 2004, 35: 2471–2485.
- [11] Ohsasa K, Matsuura K, Kurokawa K, et al. Numerical simulation of solidified structure formation of Al-Si alloy casting using cellular automaton method. *Materials Science Forum*, 2008, 575–578: 154–163.
- [12] Böttger B, Eiken J, Ohno M, et al. Controlling microstructure in magnesium alloys: a combined thermodynamic, experimental and simulation approach. *Advanced Engineering Materials*, 2006, 8(4): 241–247.
- [13] Böttger B, Eiken J, Steinbach I. Phase field simulation of equiaxed solidification in technical alloys. *Acta Materialia*, 2006, 54(10): 2697–2704.
- [14] Wang M Y, Jing T, Liu B C. Phase-field simulations of dendrite morphologies and selected evolution of primary  $\alpha$ -Mg phase during the solidification of Mg-rich Mg-Al-based alloys. *Scripta Materialia*, 2009, 61(8): 777–780.
- [15] Yuan Xunfeng, Ding Yutian, Guo Tinbiao, et al. Numerical simulation of dendritic growth of magnesium alloys using phase-filed method under forced flow. *The Chinese Journal of Nonferrous Metals*, 2010, 20(8): 1474–1480. (In Chinese)
- [16] Guo Z, Mi J, Xiong S, et al. Phase field study of the tip operating state of a freely growing dendrite against convection using a novel parallel multigrid approach. *Journal of Computational Physics*, 2014, 257: 278–297.
- [17] Yao Junping, Li Xiangguang, Long Wenyuan, et al. Numerical simulation of dendritic growth of magnesium alloys under forced flow using KKS phase-field model. *Rare Metal Materials and Engineering*, 2014, 43(1): 97–102. (In Chinese)
- [18] Wu M W, Xiong S M. Modeling of equiaxed and columnar dendritic growth of magnesium alloy. *Transactions of Nonferrous Metals Society of China*, 2012, 22(9): 2212–2219.
- [19] Wu M W, Xiong S M. A three-dimensional cellular automaton model for simulation of dendritic growth of magnesium alloy. *Acta Metallurgica Sinica (English letters)*, 2012, 25(3): 169–178.
- [20] Al-Rawahi N, Tryggvason G. Numerical simulation of dendritic solidification with convection: two-dimensional geometry. *Journal of Computational Physics*, 2002, 180(2): 471–496.
- [21] Yang Manhong, Guo Zhipeng, Xiong Shoumei. Numerical simulation of dendritic growth of magnesium alloy with convection. *The Chinese Journal of Nonferrous Metals*, 2015, 25(4): 835–843. (In Chinese)
- [22] Trivedi R, Miyahara H, Mazumder P, et al. Directional solidification microstructures in diffusive and convective regimes. *Journal of Crystal Growth*, 2001, 222(1): 365–379.